A hybrid Eulerian-Lagrangian approach for simulating liquid sprays

Fabien Evrard*, Fabian Denner, Berend van Wachem
Chair of Mechanical Process Engineering, Otto-von-Guericke University Magdeburg,
Universitätsplatz 2, 39106 Magdeburg, Germany
*Corresponding author: fabien.evrard@ovgu.de

Abstract
Interfacial flows of practical interest, of which liquid sprays are typical examples, generally involve length- and time-scales that span over several orders of magnitude. Their modelling using interface-capturing or interface-tracking methods therefore presents a prohibitively large computational cost. Over the past years, hybrid Eulerian-Lagrangian approaches have been proposed with the aim to predict the behaviour of such flows both efficiently and accurately. These approaches rely on the assumption that small, detached interfacial structures are spherical due to the dominant influence of surface tension, therefore allowing for their modelling as Lagrangian particles. The dynamics of the large interfacial structures are fully resolved on the Eulerian grid, whereas the smaller interfacial structures, resulting from breakup instances, are transferred to a Lagrangian frame of reference and tracked as point-particles. In doing so, a main issue arises due to the competing requirements of both the Eulerian and Lagrangian approaches: on the one hand, interfacial structures modelled with the Eulerian approach need to be resolved by at least a few mesh cells; and on the other hand, the accurate account of the effect of the flow on the Lagrangian particles and vice-versa requires the tracked particles to be much smaller than the Eulerian mesh cells. Interfacial structures that lie between these two limits – typically shortly before and/or after their transfer from one framework to the other – are therefore poorly represented by any of the two approaches.
In this contribution, we propose a hybrid Eulerian-Lagrangian approach that is free of such inconsistencies. It relies upon the filtering of the instantaneous flow equations with a particle marker function; a process in which a length-scale equal to a few particle diameters is chosen. This decouples the size of the Lagrangian particle with the specific length of the discrete Eulerian mesh cell in calculating the volume fraction. This filtering is also applied to the fluid-particle momentum coupling terms, which provides a solid framework for spreading these source terms. Throughout the application of the proposed method to a number of test-cases, we show that the filtering strategy allows for the consistent tracking of Lagrangian particles regardless of their size relative to the Eulerian mesh. Finally, the full hybrid framework is tested on a realistic liquid atomisation case, and the impact of the proposed filtering on the dynamics and the statistics of the spray is investigated.

Keywords
Numerical modelling, Eulerian, Lagrangian, Hybrid, Atomisation

Introduction

Despite the increase in available computational power and the advances made in interfacial flow modelling, the Direct Numerical Simulation (DNS) of atomising sprays is hardly within the reach of modern computers. In the context of interfacial flow DNS, resolving all scales requires from five to twenty mesh cells along the smallest interfacial features [1, 3]. The cost of the DNS of multi-scale interfacial flows, such as atomising sprays, is thus clearly very significant. These considerable refinement requirements have lead to the development of hybrid methods which couple interface-capturing and Lagrangian particle tracking (LPT) techniques [2, 4, 5]. The primary atomisation regime is fully resolved using an interface-capturing method, while interfacial structures deemed sufficiently small are transferred to a Lagrangian frame of reference where they are tracked based on the underlying flow field. A high level of refinement is then only required in the vicinity of the interface in the primary atomisation region, reducing the cost of the full spray atomisation simulation. The transition between the Eulerian and Lagrangian frameworks, nonetheless, proves to be delicate. One major difficulty arises from the competing mesh resolution requirements of both the Eulerian and Lagrangian approaches. The former requires a minimum of a few cells per droplet diameter, while the latter requires the droplets to be much smaller than the cells. We propose to address this issue through the filtering of the governing equations for the Eulerian phase, thereby allowing larger-than-cell Lagrangian droplets to be accurately tracked.

Material and methods

We present a hybrid Eulerian-Lagrangian framework for simulating multi-scale interfacial flows. The method is developed within a finite-volume framework with collocated variable arrangement [6], which solves in a coupled manner the incompressible Navier-Stokes equations

$$\nabla \cdot \boldsymbol{u} = 0 \,, \tag{1}$$

$$\rho \left[\frac{\partial \boldsymbol{u}}{\partial t} + \nabla \cdot (\boldsymbol{u} \otimes \boldsymbol{u}) \right] = -\nabla p + \nabla \cdot \boldsymbol{\tau} + \rho \, \boldsymbol{g} + \boldsymbol{f}_\sigma \,, \tag{2}$$

where ρ is the fluid density, $\boldsymbol{u}$ the velocity vector, p the pressure, $\boldsymbol{\tau}$ the deviatoric stress tensor, and $\boldsymbol{g}$ the gravity vector. The surface tension force $\boldsymbol{f}_\sigma$ is defined using the CSF method [8] as

$$\boldsymbol{f}_\sigma = \sigma\ \kappa\ \delta_\Gamma\ \boldsymbol{n}\ , \tag{3}$$

with σ the surface tension coefficient, κ the interface curvature, $\boldsymbol{n}$ the interface normal vector, and δ_Γ the interface density function. A volume of fluid method [7] is chosen to capture the interface motion: the gas and liquid phases are then represented implicitly by the indicator function defined as

$$\chi(\mathbf{x},t) = \begin{cases} 1 & \text{if } \mathbf{x} \in \text{liquid phase} \\ 0 & \text{if } \mathbf{x} \in \text{gas phase} \end{cases}\ . \tag{4}$$

This results in a discrete *colour function* field γ representing the fraction of liquid in each computational cell. The interface is advected based on the transport equation

$$\frac{\partial \gamma}{\partial t} + \boldsymbol{u}\nabla\gamma = 0\ , \tag{5}$$

while the density and viscosity of the fluid are obtained from the following relations

$$\rho = \rho_l\ \gamma + \rho_g(1-\gamma)\ , \tag{6}$$

$$\mu = \mu_l\ \gamma + \mu_g(1-\gamma)\ . \tag{7}$$

The subscripts g and l refer to the respective gas and liquid properties. Assuming that selected small droplets that are formed during the atomisation process remain spherical throughout the evolution of the flow, owing to the dominant effect of surface tension, they can be modelled as Lagrangian point-particles. Their motion is governed by Newton's second law, while the motion of the surrounding gas is governed by the Navier-Stokes equations. This allows to take account of the impact of the particles on the flow and vice versa without having to resolve the fluid-particle interaction at the scale of the particles.

Filtered governing equations for the Eulerian phase

In order to relax the resolution constraint associated with classical Particle-In-Cell approaches (that is: the diameter of the tracked Lagrangian particles should be much smaller than the Eulerian fluid cells – typically $d < 0.2\ \Delta x$), an approach based on local averaging is considered to model the mixture of gas and liquid droplets [9]. It relies on the definition of local mean variables and provides a sound mathematical framework for the numerical resolution of the motion of the gas/liquid mixture with particles that are similar or larger in size than the Eulerian cells. The averaging of the governing equations is achieved via convolution with a normalised filtering kernel g chosen to be

$$g(r) = \frac{21}{2\pi\delta^3} \begin{cases} (4r/\delta+1)(1-r/\delta)^4 & \text{if } 0 \le r \le \delta \\ 0 & \text{if } r > \delta \end{cases}\ , \tag{8}$$

where δ is the radius of the filter support. Using the phase indicator function χ introduced in equation (4), a local gas volume fraction is defined as

$$\varepsilon_g(\mathbf{x},t) = \int\limits_{\mathbb{R}^3} g(|\mathbf{x}-\mathbf{y}|)(1-\chi(\mathbf{y},t))\,\mathrm{d}\mathbf{y} = \int\limits_{\Omega_g(t)} g(|\mathbf{x}-\mathbf{y}|)\,\mathrm{d}\mathbf{y}\,, \tag{9}$$

where $\Omega_g(t)$ represents the portion of the three-dimensional domain occupied by the gas. The filtering of a variable ϕ results in a filtered quantity $\bar{\phi}$ such that

$$\varepsilon_g(\mathbf{x},t)\,\bar{\phi}(\mathbf{x},t) = \int\limits_{\Omega_g(t)} g(|\mathbf{x}-\mathbf{y}|)\phi(\mathbf{y},t)\,\mathrm{d}\mathbf{y}\,. \tag{10}$$

The averaging of the governing equations yields the following filtered equations

$$\frac{\partial \varepsilon_g}{\partial t} + \nabla\cdot(\varepsilon_g\boldsymbol{u}) = 0 \tag{11}$$

$$\rho\left[\frac{\partial(\varepsilon_g\boldsymbol{u})}{\partial t} + \nabla\cdot(\varepsilon_g\boldsymbol{u}\otimes\boldsymbol{u})\right] = -\varepsilon_g\nabla p + \nabla\cdot(\varepsilon_g\boldsymbol{\tau}) + \varepsilon_g\rho\boldsymbol{g} + \varepsilon_g\boldsymbol{f}_\sigma + \mathbf{M}^{\mathsf{d}} \tag{12}$$

with $\mathbf{M}^{\mathsf{d}}$ a momentum transfer term between the Eulerian and Lagrangian frameworks. Under the assumption that g varies little over a droplet diameter, $\mathbf{M}^{\mathsf{d}}$ can be simplified to

$$\mathbf{M}^{\mathsf{d}} = -\sum_d g(|\mathbf{x}-\mathbf{x}_d|)\,\boldsymbol{f}_{d,\mathsf{drag}}\ , \tag{13}$$

with $\boldsymbol{f}_{d,\mathsf{drag}}$ the drag force acting on particle d. Similarly, the gas volume fraction is obtained from

$$\varepsilon_g = 1 - \sum_d g(|\mathbf{x}-\mathbf{x}_d|)V_d\ . \tag{14}$$

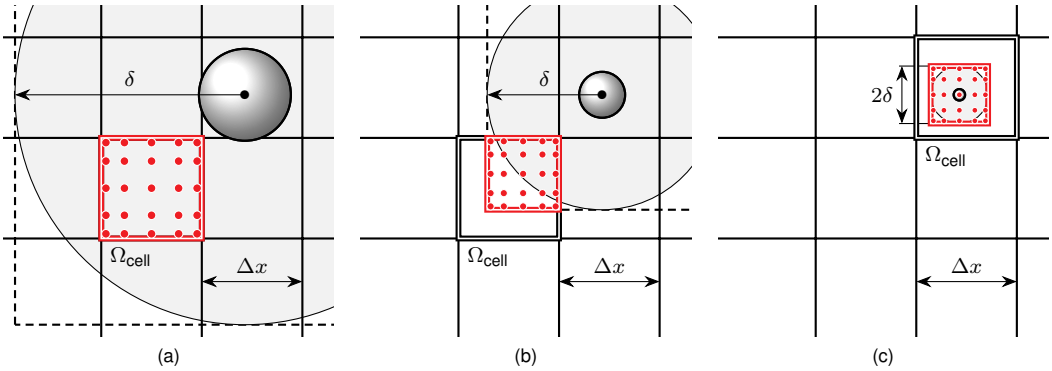

Figure 1. Computation of the discrete filter values in a finite volume formalism. The filter kernel function is integrated numerically in the intersection between each computational cell and the bounding box of the filter support. The red dots represent the numerical integration points.

Governing equations for the Lagrangian phase

In the Lagrangian frame of reference, droplets are considered as point-particles. The motion of a particle in surrounding flow is given by [10, 11]

$$\rho_l V_d \frac{\mathrm{d}\boldsymbol{u}_d}{\mathrm{d}t} = \rho_g V_d \frac{D\tilde{\boldsymbol{u}}_{g@d}}{Dt} + (\rho_l - \rho_g) V_d\, \boldsymbol{g} + \boldsymbol{f}_{d,\mathsf{drag}} + \boldsymbol{f}_{d,\mathsf{add}} + \boldsymbol{f}_{d,\mathsf{history}} \,, \tag{15}$$

where V_d is the volume of the droplet, $\boldsymbol{u}_d$ is its velocity, and $\tilde{\boldsymbol{u}}_{g@d}$ is the undisturbed gas velocity at the centre of mass of the droplet. In this study, based on the large density ratios of the considered gas-liquid flows, the following simplified solution of Newton's second law is employed:

$$\rho_l V_d \frac{\mathrm{d}\boldsymbol{u}_d}{\mathrm{d}t} = (\rho_l - \rho_g) V_d\, \boldsymbol{g} + \boldsymbol{f}_{d,\mathsf{drag}} \,. \tag{16}$$

The drag force is modelled as proposed by Wen and Yu [13],

$$\boldsymbol{f}_{d,\mathsf{drag}} = \frac{3}{4} C_\mathsf{D} \frac{V_d \rho_g}{\mathrm{d}_d\, \varepsilon_g^{1.65}} \|\tilde{\boldsymbol{u}}_{g@d} - \boldsymbol{u}_d\| (\tilde{\boldsymbol{u}}_{g@d} - \boldsymbol{u}_d) \,, \tag{17}$$

where d_d is the diameter of the droplet, and the drag coefficient C_D is based on Stokes's drag law extended with the correlation of Schiller and Naumann [12], yielding

$$C_\mathsf{D} = \begin{cases} 24\left[1 + 0.15(\varepsilon_g \mathsf{Re}_d)^{0.687}\right](\varepsilon_g \mathsf{Re}_d)^{-1} & \text{if } (\varepsilon_g \mathsf{Re}_d) \leq 1000 \\ 0.44 & \text{otherwise} \end{cases} \,. \tag{18}$$

Re_d is the Reynolds number of the droplet based on the local relative velocity, defined as

$$\mathsf{Re}_d = \frac{\rho_g \|\tilde{\boldsymbol{u}}_{g@d} - \boldsymbol{u}_d\| \mathrm{d}_d}{\mu_g} \,. \tag{19}$$

Discrete filtering

The discrete filter value in a given Eulerian cell Ω_cell, required for the computation of ε_g and $\mathbf{M}^\mathsf{d}$, is obtained by numerical integration on $\Omega_\mathsf{int} = \Omega_\mathsf{cell} \cap \Omega_{\square d}$, with $\Omega_{\square d}$ the rectangular bounding box of the sphere of radius δ centred at $\mathbf{x}_d$ (*i.e.* the bounding box of the filter support for droplet d, illustrated in Figure 1). This way, the filtered approach converges towards a classical Particle-In-Cell approach if the particle is much smaller than the Eulerian cell.

Transfers between frameworks

Separated structure identification The transfer of droplets from the Eulerian to the Lagrangian framework requires to be able to efficiently identify separated Eulerian liquid structures. The parallel algorithm of Herrmann [2] is used to that end. The properties of each liquid element are calculated by looping over the mesh cells which have the same structure id. The exact volume V_d, equivalent diameter d_d, approximate average velocity $\boldsymbol{u}_d$, and approximate center $\mathbf{x}_d$ of each liquid structure d are obtained using

$$V_d = \sum_i^d \gamma_i V_i \,, \quad \mathrm{d}_d = \left(\frac{6V_d}{\pi}\right)^{1/3} \,, \quad \boldsymbol{u}_d = \frac{1}{V_d} \sum_i^d \gamma_i \boldsymbol{u}_i V_i \,, \quad \mathbf{x}_d = \frac{1}{V_d} \sum_i^d \gamma_i \mathbf{x}_i V_i \,, \tag{20}$$

where Σ_i^d represent the summation over all cells marked with the id of structure d, and γ_i, V_i, $\boldsymbol{u}_i$, and $\mathbf{x}_i$ are the colour function, volume, velocity, and center for the i^th Eulerian mesh cell.

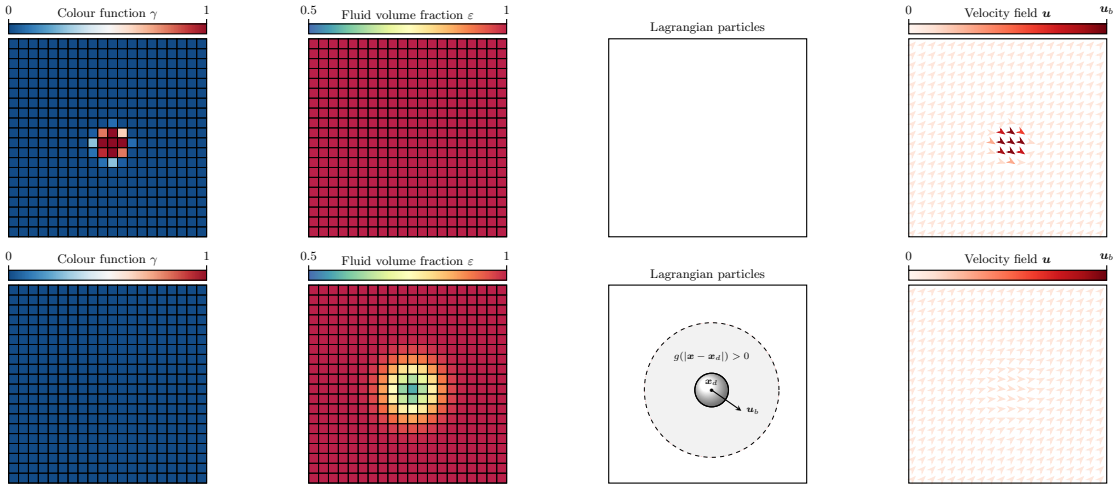

Figure 2. Illustration of the Eulerian to Lagrangian conversion of a liquid droplet. The colour function, velocity, and volume fraction Eulerian fields are updated while a Lagrangian particle is injected. Top row: Before Eulerian to Lagrangian conversion; Bottom row: After Eulerian to Lagrangian conversion.

Conversion criteria The Lagrangian tracking of the liquid droplets relies upon the assumption that these droplets are and stay spherical during their transport. Physical models, for instance based on the critical Weber number, can be used to verify that the Lagrangian tracking can be employed. Additionally, numerical considerations come into play when deciding whether Eulerian liquid structures should be transferred to a Lagrangian representation. The degree of refinement with which a given liquid structure is resolved on the Eulerian mesh is a very important criterion. Eulerian droplets which are resolved by less than two to five cells along their diameter are typically inaccurately represented [1]. A threshold volume criterion V_{cut} is thus usually introduced: if the volume V_d of a separated Eulerian liquid structure is such that $V_d < V_{\text{cut}}$, then the structured is transferred to the Lagrangian framework, regardless of its Weber number. Other criteria involving the aspect ratio of the droplet, internal fluctuating energy, or the proximity of the droplet to other larger liquid structures, may also be considered [2, 4, 5]. Ultimately, transfer criteria should be chosen based on the level of sophistication of the LPT method employed and on the highest degree of refinement which can be reached on the Eulerian grid.

Transfer from Eulerian to Lagrangian framework The transfer of a liquid element from the Eulerian to the Lagrangian framework consists of the following steps, illustrated in Figure 2:

Step 1. The colour function field component associated with the liquid structure is set to zero.

Step 2. A Lagrangian droplet with diameter d_d and velocity $\boldsymbol{u}_d$ is injected at the center $\mathbf{x}_d$ of the liquid structure.

Step 3. The volume fraction contribution of the Lagrangian particle is updated.

Step 4. The newly injected particle should see the undisturbed gas velocity field $\tilde{\boldsymbol{u}}$ for the drag law in Eq. (17) to be applicable. Therefore, the motion of the surrounding gas due to the droplet's presence is removed from the Eulerian framework using the following weighted interpolation:

$$\tilde{\boldsymbol{u}}_i = \frac{\sum\limits_j \boldsymbol{u}_j [1 - \phi^{\mathsf{W}}_{\delta_d}(|\mathbf{x}_j - \mathbf{x}_d|)]^3 \phi^{\mathsf{W}}_{\delta_d}(|\mathbf{x}_j - \mathbf{x}_i|)}{\sum\limits_k [1 - \phi^{\mathsf{W}}_{\delta_d}(|\mathbf{x}_k - \mathbf{x}_d|)]^3 \phi^{\mathsf{W}}_{\delta_d}(|\mathbf{x}_k - \mathbf{x}_i|)} \,, \tag{21}$$

where $\mathbf{x}_i$ is the center of the i^{th} Eulerian mesh cell, and $\phi^{\mathsf{W}}_{\delta_d}$ is the radial basis function used in the filter kernel. The combination of the two weights $[1 - \phi^{\mathsf{W}}_{\delta_d}(|\mathbf{x} - \mathbf{x}_d|)]^3$ and $\phi^{\mathsf{W}}_{\delta_d}(|\mathbf{x} - \mathbf{x}_i|)$ in Eq. (21) allows the undisturbed velocity to be interpolated from the local velocities weighted by their non-proximity to the centre of the removed Eulerian liquid structure.

Transfer from Lagrangian to Eulerian framework Lagrangian droplets may have to be transferred back to an Eulerian representation as their trajectory brings them towards the Eulerian gas-liquid interface. This transfer consists of the following steps:

Step 1. The colour function field is updated with the contribution of the liquid droplet.

Step 2. The droplet is removed from the Lagrangian framework.

Step 3. The volume fraction contribution of the Lagrangian particle is removed from the Eulerian framework.

Step 4. The momentum contribution of the droplet is transferred to the Eulerian framework by updating the velocity field following

$$\boldsymbol{u}_{i,\text{new}} = \frac{\rho_g \boldsymbol{u}_i + \rho_l \gamma_i \boldsymbol{u}_d}{(1-\gamma_i)\rho_g + \gamma_i \rho_l} \,, \tag{22}$$

where $\boldsymbol{u}_{i,\text{new}}$ is the updated velocity in the i^{th} cell, and γ_i the colour function contribution resulting from the transfer of the droplet d.

Volume-fraction-related constraints The account of the gas volume fraction contribution in the governing flow equations adds supplementary constraints to the hybrid approach. When ε_g is not constant, the filtered flow equations do not necessarily yield a divergence-free velocity field, resulting in an artificial gain or loss of liquid during the VOF transport. Lagrangian particles must thus be located far-enough from the interface for their volume fraction contribution not to introduce mass errors. An additional distance-related transfer criterion is then introduced. For a structure to be eligible for transfer, one must have

$$\|\mathbf{x}_d - \mathbf{x}_\Gamma\| > \delta + \frac{3\sqrt{3}}{2}\Delta x \,, \tag{23}$$

where $\mathbf{x}_d$ is the centre of mass of the liquid structure, and $\mathbf{x}_\Gamma$ represents the centers of all Eulerian mesh cells where $\gamma > 0$. The same criterion is used to transfer a Lagrangian droplet back to the Eulerian framework when it is moving towards the gas-liquid interface.

Results and discussion

The proposed hybrid approach is applied to simulate an atomising spray in a swirl injector configuration, based on the experiment conducted in [14]. The liquid (ethanol) is injected into a quiescent gas (air) with a swirl component originating from the geometry of the injector. Simulations are conducted on a $200 \times 400 \times 400$ Cartesian grid, meaning that the annulus' outer diameter d is resolved by 21 cells. The simulations cannot be considered as direct numerical simulations, as it is clear that the smallest liquid structures are not properly resolved. However, they provide valuable information with regard to the impact of the proposed hybrid Eulerian-Lagrangian approach on the dynamics of the interface and the spray statistics.

The simulations are conducted using (a) a purely Eulerian approach (using the VOF interface-capturing method), (b) the hybrid Eulerian-Lagrangian approach using a simplified filtered approach [4] (referred to as "two-way coupling"), and (c) the hybrid Eulerian-Lagrangian approach using the proposed approach (referred to as "three-way coupling"). Droplets are considered suitable candidates for their transfer from the Eulerian to the Lagrangian framework if their volume V_d is smaller than a threshold volume V_{cut} equal to the volume of a sphere with diameter $d_{\text{cut}} = 3\,\Delta x$. In addition to this criterion, the distance criterion $\|\mathbf{x}_d - \mathbf{x}_\Gamma\| > \delta + 3\sqrt{3}\,\Delta x/2$ is used.

Figure 3 presents snapshots of the three-way coupled simulation showing both Eulerian and Lagrangian phases, the Eulerian phase alone, and the Lagrangian phase alone. Figures 4 and 5 illustrate the transfer of droplets between Eulerian and Lagrangian frameworks. In Figure 4, a set of small Eulerian droplets resulting from the break up of a liquid filament is transferred to the Lagrangian framework. In Figure 5, a Lagrangian droplet moving towards the Eulerian fluid-fluid interface is converted back to a Eulerian representation, and later on merges with.

The impact of the type of coupling employed on various statistics of the flow becomes evident in Figure 6. For instance, Figure 6 shows the evolution of the individual Lagrangian droplet velocities $\|U_d\|$ normalised by the velocity of the considered droplet at the time t_{inject} of its injection into the Lagrangian framework. From the average velocity evolutions, it appears that with the two-way coupling approach, Lagrangian droplets are subject to less deceleration than with the three-way coupling approach, an under-estimation of drag which is frequently observed for large particles in classical Euler-Lagrangian frameworks.

Conclusions

We have presented a hybrid Eulerian-Lagrangian approach, combining a Volume-of-Fluid (VOF) interface-capturing method with Lagragian Particle Tracking (LPT). Large-scale interfacial features are fully resolved with the interface-capturing scheme, whereas small-scale interfacial features are tracked based on a simplified Lagrangian model. An enhanced Lagrangian framework which relies on local averaging and enables the consideration of arbitrary particle-size to cell-size ratios has been proposed. The proposed approach is tested several cases, including a realistic spray atomisation case. The simulations provide valuable information with regard to how the proposed approach compares against a simplified approach which neglects the contribution of the gas volume fraction in the governing flow equations, as well as against a fully Eulerian approach.

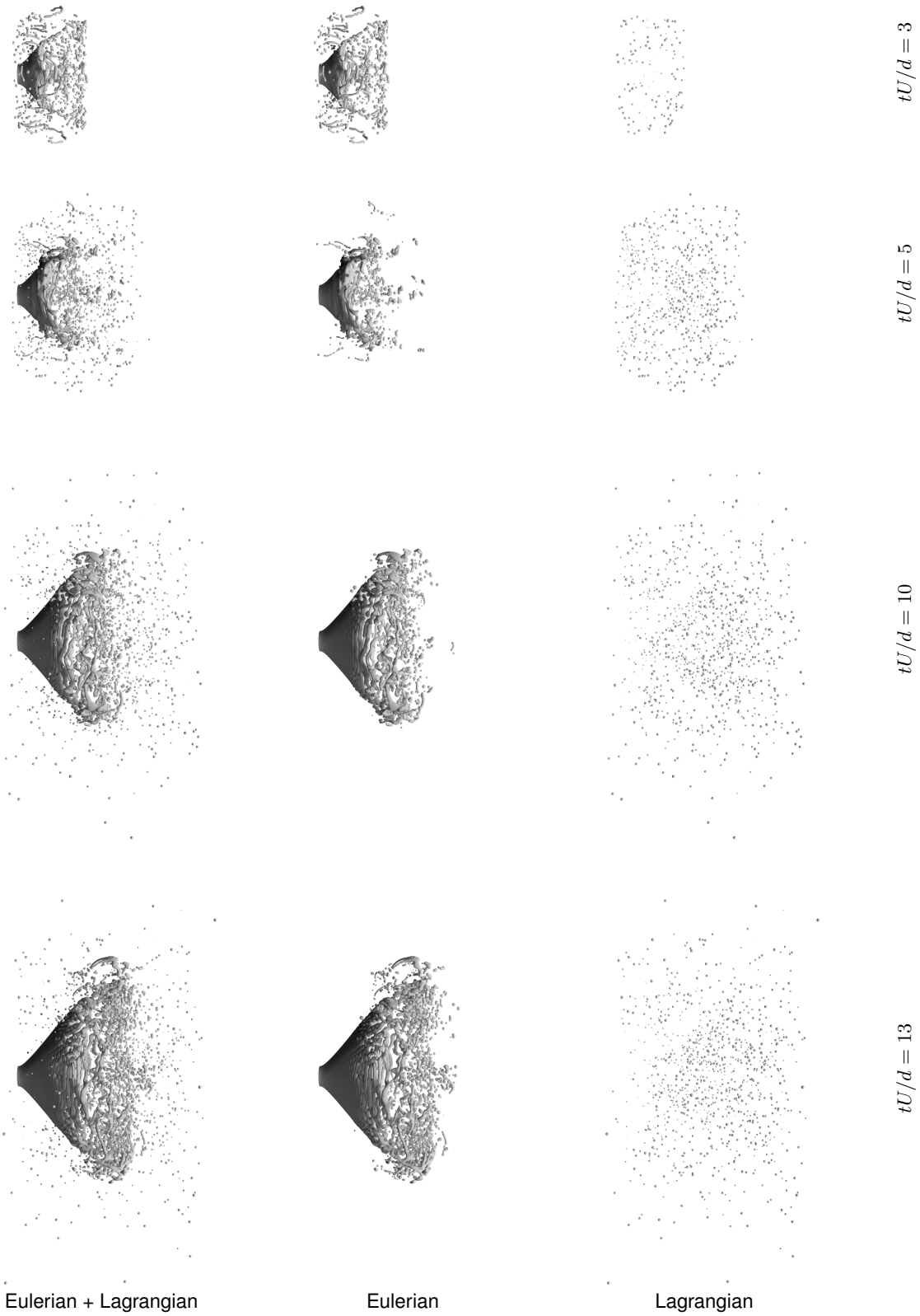

Figure 3. Snapshots of the swirl atomiser spray simulations using the proposed hybrid approach with three-way coupling, showing both Eulerian and Lagrangian phases, the Eulerian phase alone, and the Lagrangian phase alone.

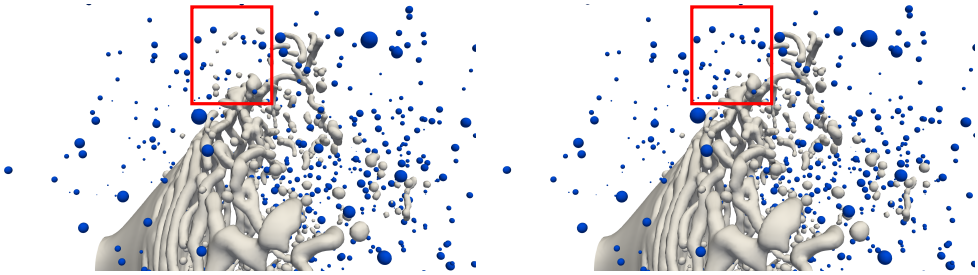

(a) t (b) $t + \Delta t$

Figure 4. Illustration of the Eulerian to Lagrangian transfer using the proposed hybrid VOF-LPT approach. Lagrangian droplets are represented by blue spheres, and the Eulerian liquid interface is represented as the $\gamma = 0.1$ iso-contour. Examples of Eulerian liquid structures which are transferred to the Lagrangian framework between the time-steps **(a)** and **(b)** can be observed in the highlighted red frame.

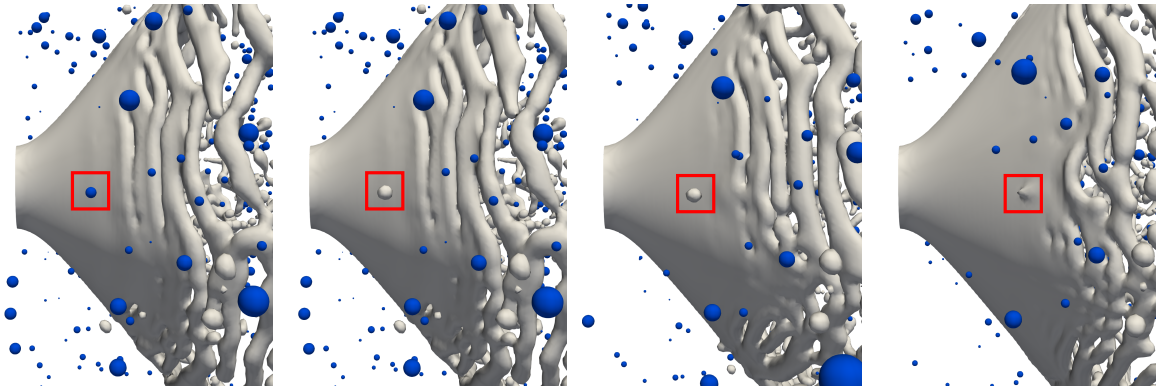

(a) t (b) $t + \Delta t$ (c) $t + 50\Delta t$ (d) $t + 100\Delta t$

Figure 5. Illustration of the Lagragian to Eulerian transfer using the proposed hybrid VOF-LPT approach. Lagrangian droplets are represented by blue spheres, and the Eulerian liquid interface is represented as the $\gamma = 0.1$ iso-contour. The droplet highlighted in the red frame is transferred from the Lagrangian framework back to an Eulerian representation as it comes closer to the Eulerian interface. It ultimately collides and merges with it.

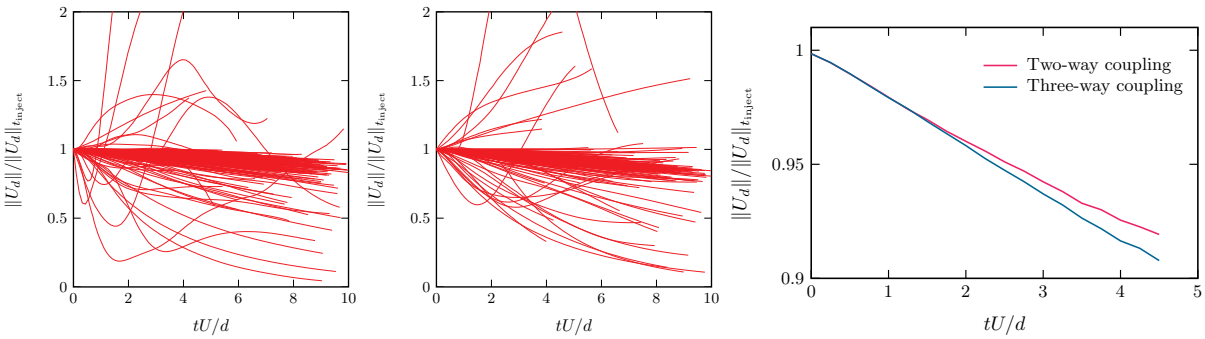

(a) Two-way coupling (b) Three-way coupling (c) Average velocities

Figure 6. Evolution of the individual Lagrangian droplet velocities normalised by the velocity of the droplet at the time of its injection into the Lagrangian framework, using **(a)** two-way coupling and **(b)** three-way coupling. The resulting average velocities are shown in **(c)**

References

[1] M. Gorokhovski, M. Herrmann, Modeling Primary Atomization, Annual Review of Fluid Mechanics 40 (2008) 343–366.
[2] M. Herrmann, A parallel Eulerian interface tracking/Lagrangian point particle multi-scale coupling procedure, Journal of Computational Physics 229 (2010) 745–759.
[3] M. Herrmann, On Simulating Primary Atomization Using The Refined Level Set Grid Method, Atomization and Sprays 21 (2011) 283-301.
[4] Y. Ling, S. Zaleski, R. Scardovelli, Multiscale Simulation of Atomization with Small Droplets Represented by a Lagrangian Point-Particle Model, International Journal of Multiphase Flow 76 (2015) 122–143.
[5] D. Zuzio, J.-L. Estivalèzes, B. DiPierro, An improved multi-scale Eulerian–Lagrangian method for simulation of atomization process, Computers & Fluids (2016).
[6] F. Denner, B. van Wachem, Fully-coupled balanced-force VOF framework forarbitrary meshes with least-squares curvature evaluation from volume fractions, Numerical Heat Transfer Part B: Fundamentals 65 (2014) 218–255.
[7] C. Hirt, B. Nichols, Volume of fluid (VOF) method for the dynamics of free boundaries, Journal of Computational Physics 39 (1981) 201–225.
[8] J. Brackbill, D. Kothe, C. Zemach, Continuum Method for Modeling Surface Tension, Journal of Computational Physics 100 (1992) 335–354.
[9] T. B. Anderson, R. O. Y. Jackson, A fluid mechanical description of fludized beds, I&EC Fundamentals 6 (1967) 524–539.
[10] M. R. Maxey, J. R. J. Riley, Equation of motion for a small rigid sphere in a nonuniform flow, Physics of Fluids 26 (1983) 883.
[11] R. Gatignol, The Faxén formulas for a rigid particle in an unsteady non-uniform Stokes-flow, Journal de Mécanique théorique et appliquée 2 (1983) 143–160.
[12] L. Schiller, A. Naumann, Uber die grundlegenden Berechnungen bei der Schwerkraftaufbereitung, Ver. Deut. Ing 77 (1933) 318–320.
[13] C. Wen, Y. Yu, Mechanics of fluidization, The Chemical Engineering Progress Symposium Series 62 (1966) 100–111.
[14] H. Correia Rodrigues, M. J. Tummers, E. H. van Veen, D. J. Roekaerts, Spray flame structure in conventional and hot-diluted combustion regime, Combustion and Flame 162 (2015) 759–773.